Phase Diagrams and Phase Separation Dynamics in Mixtures of Side-Chain Liquid Crystalline Polymers and Low Molar Mass Liquid Crystals

Hao-Wen Chiu, Zheng Long Zhou, and Thein Kyu*

Institute of Polymer Engineering, The University of Akron, Akron, Ohio 44325-0301

Leonorina G. Cada and L.-C. Chien

Liquid Crystal Institute, Kent State University, Kent, Ohio 44242

Received August 15, 1995; Revised Manuscript Received November 6, 1995[⊗]

ABSTRACT: Miscibility phase diagrams and phase separation dynamics in mixtures of side-chain liquid crystalline polymers (SCLCP) and monomeric liquid crystals have been investigated experimentally in order to test with theoretical predictions. The theoretical calculation on equilibrium phase diagrams of binary nematic mixtures involves a combination of the Flory−Huggins (FH) free energy for isotropic mixing in conjunction with the Maier−Saupe (MS) free energy for nematic ordering of the mesogenic units. Two orientational order parameters and two nematic−isotropic (NI) transitions of the constituent mesogens are taken into consideration in the calculation. This combined FH−MS theory predicts a variety of phase diagrams depending on the relative strength of the cross-interaction between two dissimilar mesogens as compared to that in the same species. A series of epoxy resins [ethylene glycol glycidyl ether (EGDE)] grafted with mesogenic amines 4-(ω-aminoalkoxy)-4′-cyanobiphenyl were synthesized. The temperature−composition phase diagrams of these SCLCP mixtures and the eutectic low molar mass liquid crystal (E7) have been established by a cloud point method. The calculated phase diagrams are found to accord well with the experimental phase diagrams. The dynamics of phase separation has been investigated by means of time-resolved light scattering and optical microscopy. The time evolution of the structure factor following various temperature quenches into the nematic−liquid and/or nematic−nematic coexistence regions has been analyzed in terms of a power law scheme.

Introduction

Side-chain liquid crystalline polymers (SCLCP) have been synthesized for use as matrix resins in polymer dispersed liquid crystals (PDLC) in order to improve the wide-angle viewability and optical transmittance in the on-state of the applied electric field. The refractive index of the mesogens of low molecular weight liquid crystals (LC) is customarily matched with that of the mesogenic side groups of the SCLCP so that the refractive index appears the same from all viewing angles.[1,2] PDLC is basically an inhomogeneous composite film comprising low molecular weight LC dispersed in a polymer matrix which may be prepared by polymerization or thermally induced phase separation from an initially homogeneous state.[1] The electro-optical performance of these PDLC materials depends strongly on domain size, shape, uinformity, and dispersion as well as topology (configuration) of the LC within the dispersed domains. The size (length scale) and shape of the liquid crystal domains are generally determined by both thermodynamics and kinetics of phase separation during preparation processes.[1]

In order to gain insight into the structure of dispersed LC domains and to critically match the refractive index of the side-chain liquid crystalline polymers with that of the low molar mass LC, we have synthesized a series of epoxy resins [ethylene glycol diglycidyl ether (EGDE) grafted with mesogenic amines 4-(ω-aminoalkoxy)-4′-cyanobiphenyl connected by various methylene linkages (EGDE-C*x*, where *x* is the number of methylene carbons).[3] The dispersing low molar mass LC is the eutectic liquid crystal mixture consisting of cyanobiphenyl derivatives, commercially known as E7. We first examined the phase behavior for the mixtures of these epoxy polymers and E7 by establishing various phase diagrams of EGDE-C*x*/E7 mixtures where $x = 6-9$. We then investigated the structure evolution during thermal quenching from single-phase to two-phase regions, viz., nematic−liquid and nematic−nematic coexistence regions. The phase equilibria and dynamical behavior of phase separation in these systems have been analyzed by combining the Flory−Huggins (FH) theory for isotropic mixing[4,5] and the Maier−Saupe (MS) theory of nematic ordering.[6−8]

Phase Diagram Calculations

The combined FH/MS theory under consideration is basically a mean-field model in which the stability of the nematic phase is assumed to arise from the repulsive interaction of the mesogenic groups.[6−8] The rigidity of polymer chains is not considered here, as it may be insignificant for side-chain liquid crystalline polymers, although it might be important for main-chain liquid crystalline polymers. Other transitions associated with crystal and smectic phases as well as glass transitions, even if they exist, are ignored in the present calculation.

In the combined FH/MS theory, the total free energy for binary nematic mixtures is customarily described in terms of a simple addition of the free energy of mixing of isotropic liquids, g^{i}, and the free energy of nematic ordering of liquid crystals, g^{n}, i.e.,

$$g = g^{i} + g^{n} \tag{1}$$

where g represents the dimensionless total free energy density of the system.

The free entropy of isotropic mixing of a binary polymer blend may be expressed in terms of the Flory−

* To whom correspondence should be addressed.

[⊗] Abstract published in *Advance ACS Abstracts,* January 15, 1996.

0024-9297/96/2229-1051$12.00/0

Huggins theory;[4,5] viz.,

$$g^{\mathrm{i}} = \frac{G^{\mathrm{i}}}{nkT} = \frac{\phi_1}{r_1} \ln \phi_1 + \frac{\phi_2}{r_2} \ln \phi_2 + \chi \phi_1 \phi_2 \qquad (2)$$

where k is the Boltzmann constant and T is the absolute temperature. r_1 is the number of sites occupied by one liquid crystal molecule and is equal to unity for a low molar mass liquid crystal, where r_2 represents the number of sites or segments occupied by a single liquid crystalline polymer chain. ϕ_1 and ϕ_2 represent the volume fractions of components 1 and 2, respectively. $n = n_1 r_1 + n_2 r_2$, where n_1 and n_2 are the numbers of liquid crystal and liquid crystalline polymer molecules, respectively. χ is known as the Flory−Huggins interaction parameter which is generally assumed to be a function of reciprocal absolute temperature, i.e., $\chi = A + B/T$, where A and B are constants.[5]

The contribution of nematic ordering to the total free energy of binary nematic mixtures is generally given by the Maier−Saupe mean-field theory.[6−8] Following a theoretical scheme of Brochard et al.,[9] the free energy density of binary nematic mixtures containing side-chain liquid crystalline polymers and/or low molar mass liquid crystals may be described as

$$g^{\mathrm{n}} = \frac{G^{\mathrm{n}}}{nkT} = -\Sigma_1 \phi_1 - \Sigma_2 \phi_2 - \frac{1}{2}\nu_{11} s_1^{\,2} \phi_1^{\,2} - \frac{1}{2}\nu_{22} s_2^{\,2} \phi_2^{\,2} - \nu_{12} s_1 s_2 \phi_1 \phi_2 \qquad (3)$$

where Σ_1 and Σ_2 represent the decrease of entropy due to the alignment of individual LC molecules of component 1 and the mesogenic group of component 2, respectively. ν_{11} and ν_{22} are the nematic interaction parameters of the pure components whereas ν_{12} represents the cross-nematic interaction between the dissimilar mesogens. The self-consistent orientational order parameters s_1 and s_2 are further defined as[6]

$$s_j = \frac{1}{2}(3\langle \cos^2 \theta_j \rangle - 1) \qquad (4)$$

in which θ_j is the angle between the director of a liquid crystal molecule belonging to component j ($j = 1$ or 2) and the reference axis. The angle brackets, $\langle\rangle$, denote the ensemble average which is defined as

$$\langle \cos^2 \theta_j \rangle = \int \cos^2 \theta_j f(\theta_j) \, \mathrm{d} \cos \theta_j \qquad (5)$$

Here, $f(\theta_j)$ represents the normalized orientation distribution function and is considered to be symmetric around the reference axis, which can be expressed by

$$f(\theta_j) = \frac{1}{4\pi Z_j} \exp\left[-\frac{u(\theta_j)}{kT}\right] \qquad (6)$$

where Z_j is the partition function defined as

$$Z_j = \int \exp\left[-\frac{u(\theta_j)}{kT}\right] \mathrm{d} \cos \theta_j \qquad (7)$$

and $u(\theta_j)$ is the potential field of a director orientation which can be taken to be proportional to the second-order Legendre polynomials, i.e.,

$$\frac{u(\theta_j)}{kT} = -\frac{1}{2} m_j (3 \cos^2 \theta_j - 1) \qquad (8)$$

in which m_j is a dimensionless mean-field parameter characterizing the strength of the potential field.[8]

The order parameter, s_j, can then be related to Z_j through

$$s_j = \int f(\theta_j) \frac{1}{2}(3 \cos^2 \theta_j - 1) \, \mathrm{d} \cos \theta_j = \frac{1}{Z_j} \frac{\mathrm{d}Z_j}{\mathrm{d}m_j} \qquad (9)$$

and the entropy Σ_j can be deduced as

$$\Sigma_j = -\int f(\theta_j) \ln[4\pi f(\theta_j)] \, \mathrm{d}\Omega_j = \ln Z_j - m_j s_j \qquad (10)$$

where Ω_j denotes the solid angle. In a previous paper,[10] the nematic interaction parameters, ν_{11} and ν_{22}, of the individual mesogenic component have been shown to have an inverse temperature dependence as follows:

$$\nu_{jj} = 4.541 \frac{T_{\mathrm{NI,j}}}{T} \qquad (11)$$

The exact relation of ν_{12} to ν_{11} and ν_{22} is usually not known; we thus assume that $\nu_{12} = \nu_{21}$ and ν_{12} is proportional to the square root of the product of ν_{11} and ν_{22}, i.e.,[11]

$$\nu_{12} = c\sqrt{\nu_{11}\nu_{12}} \qquad (12)$$

where c is the proportionality constant characterizing the relative strength of the cross-interaction between the two dissimilar mesogens as compared to that in the same mesogens. The stability limit of the system can be established by calculating the chemical potentials of each component, i.e., taking the first derivative of the free energy of the system with respect to the number of molecules of each component. Similar to the free energy of mixing, the total chemical potential of mesogenic mixtures is contributed by the isotropic mixing and the nematic ordering, i.e., $\mu_j = \mu_j^{\mathrm{i}} + \mu_j^{\mathrm{n}}$. The chemical potentials resulting from the isotropic mixing can be derived to give

$$\frac{\mu_1^{\mathrm{i}}}{kT} = \ln \phi_1 + \left(1 - \frac{r_1}{r_2}\right)\phi_2 + \chi r_1 \phi_2^{\,2} \qquad (13)$$

$$\frac{\mu_2^{\mathrm{i}}}{kT} = \ln \phi_2 + \left(1 - \frac{r_2}{r_1}\right)\phi_1 + \chi r_2 \phi_1^{\,2} \qquad (14)$$

and the chemical potentials due to the nematic ordering can be deduced as

$$\frac{\mu_1^{\mathrm{n}}}{kT} = \frac{1}{2} r_1 \nu_{11} s_1^{\,2} \phi_1^{\,2} + \frac{1}{2} r_1 \nu_{22} s_2^{\,2} \phi_2^{\,2} + r_1 \nu_{12} s_1 s_2 \phi_1 \phi_2 - r_1 \ln Z_1 \qquad (15)$$

$$\frac{\mu_2^{\mathrm{n}}}{kT} = \frac{1}{2} r_2 \nu_{11} s_1^{\,2} \phi_1^{\,2} + \frac{1}{2} r_2 \nu_{22} s_2^{\,2} \phi_2^{\,2} + r_2 \nu_{12} s_1 s_2 \phi_1 \phi_2 - r_2 \ln Z_2 \qquad (16)$$

By equating the chemical potentials of each component in the individual phase and solving simultaneous equations for various temperatures, the binodal curves can be determined.

Further, the equilibrium coexistence points to a given temperature can be determined by a double tangent method where the equilibrium volume fractions of the individual phase (ϕ^{I} and ϕ^{II}) fall on the same tangent

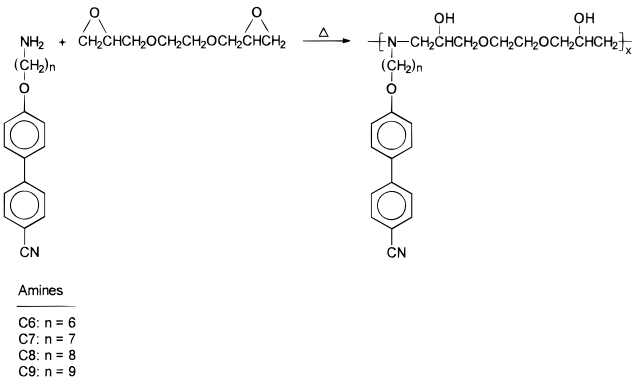

Figure 1. Synthesis scheme of the side-chain liquid crystalline polymers.

line of the free energy curve. The first derivatives of the total free energy with volume fraction are equivalent at these two compositions and also equal to the slope connecting these two points, i.e.,

$$\frac{g^{\mathrm{I}} - g^{\mathrm{II}}}{\phi^{\mathrm{I}} - \phi^{\mathrm{II}}} = \left(\frac{\partial g}{\partial \phi}\right)^{\mathrm{I}} \tag{17}$$

$$\frac{g^{\mathrm{I}} - g^{\mathrm{II}}}{\phi^{\mathrm{I}} - \phi^{\mathrm{II}}} = \left(\frac{\partial g}{\partial \phi}\right)^{\mathrm{II}} \tag{18}$$

The first derivative of total free energy of the system with volume fraction of component 1 can be deduced to give

$$\frac{\partial g}{\partial \phi_1} = \frac{1}{r_1} \ln \phi_1 - \frac{1}{r_2} \ln \phi_2 + \frac{1}{r_1} - \frac{1}{r_2} + \chi(1 - 2\phi_1) + \ln \frac{Z_2}{Z_1} \tag{19}$$

Regarding the detailed calculations of the phase diagrams, the interested readers are referred to our previous paper.[11]

Experimental Section

Ethylene glycol diglycidyl ether (EGDE) was obtained from Aldrich Chemical Co. and used as received. Mesogenic amines C6, C7, C8, and C9 were synthesized in our laboratory; the detailed synthesis scheme has been reported elsewhere.[3] The side-chain liquid crystalline epoxies EGDE-C6, EGDE-C7, EGDE-C8, and EGDE-C9 were synthesized by a ring-operating reaction of EGDE with mesogenic amines, are shown in Figure 1. Equivalent amounts of the EGDE and amine were charged into a polymerization vessel purged with circulating dry nitrogen. The reaction mixture was then heated in an oil bath at 120 °C for 24 h. The resulting polymers were purified by dissolving in tetrahydrofuran (THF) and subsequently precipitating into a 3:1 mixture of petroleum ether and ethyl ether. The same process was repeated three times, and the final precipitates were dried in a vacuum oven at room temperature for 48 h.

The dispersing liquid crystal, commercially called E7, was purchased from EM Industries. E7 is a mixture of small molecule mesogens consisting of 51 wt % 4′-*n*-pentyl-4-cyanobiphenyl (5CB), 21 wt % 4′-*n*-heptyl-4-cyanobiphenyl (7CB), 16 wt % 4′-*n*-octoxy-4-cyanobiphenyl (8OCB), and 12 wt % 4′-*n*-pentyl-4-cyanoterphenyl (5CT). The composition of E7 appears complex; however, it exhibits a single NI transition at 60 °C and a single crystal−nematic (KN) transition at −30 °C. Because of this eutectic behavior, the mixtures of the side-chain liquid crystalline epoxy polymers and E7 may be regarded as quasi-binary systems. Also, the broad nematic range (−30 to +60 °C) makes E7 a preferred choice as compared to a single component liquid crystal such as 5CB which has a NI transition temperature very close to the KN transition temperature.[12]

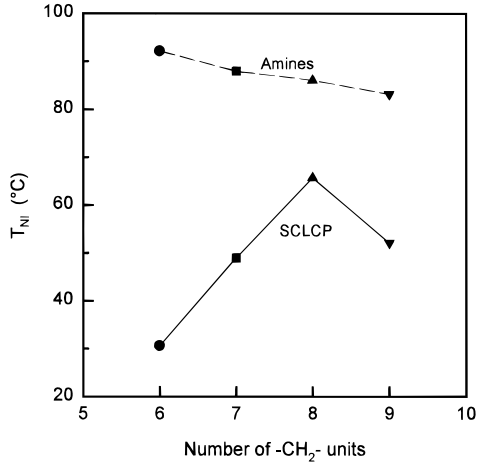

Figure 2. Effect of spacer length on the nematic isotropic transition temperatures of the mesogenic amines and thus synthesized side-chain liquid crystalline polymers.

Various ratios of side-chain liquid crystalline epoxy polymers grafted with mesogenic amine side groups (EGDE-C6, EGDE-C7, EGDE-C8, and EGDE-C9) and liquid crystal E7 were dissolved together in tetrahydrofuran (THF) and stirred vigorously at ambient temperature. The solutions were then solvent cast onto glass slides. The thin films (about 10 μm thick) thus formed were heated on a heating block at 90 °C for 10 min and then a cover glass was placed on the sample. The whole assembly was put into a vacuum oven at room temperature for 24 h to ensure the complete removal of the solvent.

The nematic−isotropic (NI) transition temperatures of the mesogenic amines and the side-chain liquid crystalline epoxy polymers were measured by a light scattering method. The temperature versus composition phase diagrams of EGDE-C6/E7, EGDE-C7/E7, EGDE-C8/E7, and EGDE-C9/E7 mixtures were established through the cloud point measurements by monitoring the scattered intensity at a given scattering angle (∼20°) using a silicon photodiode detector (HC-220-01, Hamamatsu Co.). A randomly polarized 2 mW He−Ne laser (LSR2R, Aerotech) with a wavelength of 632.8 nm was used as the incident light source. A programmable temperature controller (Model CN-2012, Omega) with a resolution of ±0.1 deg was utilized for temperature scans. The heating and cooling rate was 0.5 °C/min unless indicated otherwise. The structure evolution process of phase separation was followed by the time-resolved light scattering technique and optical microscopy. The scattering profile (scattered intensity versus scattering wavenumbers) was measured by a one-dimensional silicon diode Reticon detector (Model 1453, Princetone Applied Research) coupled with an optical multichannel analyzer (OMA III, EG & G). A two-dimensional scattering pattern was acquired by a charge-coupled detector (CCD) (Model 1430P, Princeton Applied Research). The details of the light scattering apparatus were reported elsewhere.[13] A polarizing optical microscope (a Nikon Optiphot 2-pol) equipped with polarizers and a halogen light source (12 V, 100 W) was utilized to determine the coexistence regions such as liquid−liquid, nematic−liquid, etc. by monitoring the structure change during heating and cooling cycles.

Results and Discussion

Phase Transitions of Mesogens. Figure 2 illustrates the nematic−isotropic (NI) transition temperatures of the mesogenic amines with varying spacer units (C6, C7, C8, and C9) and the side-chain liquid crystalline epoxy polymers (EGDE-C6, EGDE-C7, EGDE-C8, and EGDE-C9) derived from the reaction of these mesogens with EGDE. The NI transition temperatures of the amines decrease with increasing spacer (−[−CH_2−]$_n$−) length, which is explicable by the de-

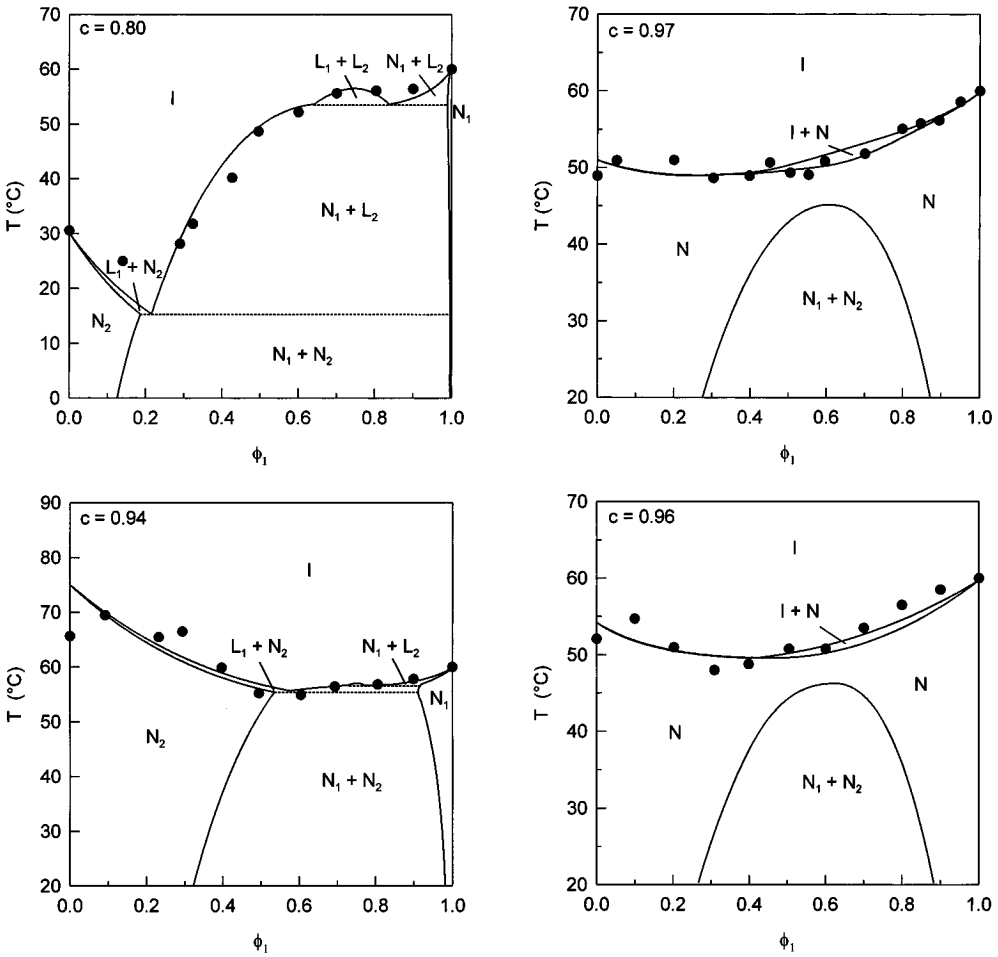

Figure 3. Temperature versus composition phase diagrams for (a) EGDE-C6/E7, (b) EGDE-C7/E7, (c) EGDE-C8/E7, and (d) EGDE-C9/E7 mixtures in comparison with the theoretical phase diagrams calculated using the various *c* values indicated (solid lines).

crease of the intermolecular attraction force between the terminal amino group and the aromatic centers as well as the reduced packing entropy resulting from the steric intermolecular repulsion in the longer chain species.[14,15] The odd−even effect of methylene spacers has been reported for main-chain as well as side-chain liquid crystals[7] in that the nematic ordering appears more stable for the even-numbered spacers relative to the odd-numbered spacer units. This effect has been attributed to the greater stabilization by the even spacer units. In the pure mesogens, the NI transitions of C6 and C8 show greater stability relative to that of mesogens with odd spacer units such as C7 and C9, but the odd−even effect is not very pronounced.

When these mesogens were grafted onto the backbone polymer chains, the NI transition temperatures of the side-chain liquid crystalline epoxy polymers are usually depressed as compared to that of the pure mesogenic amines. This lowering of NI transition temperatures may be caused by the steric constraint imposed by the backbone polymer onto the mesogenic ordering. This effect would be severe especially for short methylene linkages such as EGDE-C6. With increasing spacer length, the mesogenic side groups may be decoupled from the backbone polymer so that the NI transition temperature of the SCLCP tends to increase and approaches the original NI transitions of the pure mesogens. At a glance, it seems there is no correlation between the spacer length of the mesogenic amines and the NI transition temperatures of the side-chain liquid crystalline polymers. However, if one ignores the NI transition of the EGDE-C6 which is severely suppressed by the backbone polymer, the even-numbered SCLCP (EGDE-C8) appears more stable than the odd numbers (EGDE-C7 and EGDE-C9).

Phase Diagrams of Nematic Mixtures. The temperature versus composition phase diagrams of the side-chain liquid crystalline epoxy polymers/liquid crystals mixtures are usually complex and depend strongly on the nematic−isotropic transition temperatures of both components and, especially, the relative strength of cross-nematic interactions between them. The phase diagram calculations were carried out in comparison with the experimental phase diagrams of the EGDE-C6/E7, EGDE-C7/E7, EGDE-C8/E7, and EGDE-C9/E7 systems by assuming the densities of the side-chain liquid crystalline polymers and E7 to be equivalent, as shown in Figure 3a−d, respectively.

Figure 3a depicts the cloud point temperatures of the EGDE-C6/E7 system along with the calculated phase diagram (solid lines). The *c* parameter, which accounts for the relative strength of the cross-nematic interaction to that in the same species, was set to 0.8 and the $r_2/r_1 = 9/1$ (analogous to their molecular weight ratio). The temperature dependence of χ may be estimated by choosing an appropriate *A* value (−1.0 in the present case) to account for the broadness of the temperature versus composition curve. The *B* value in turn may be estimated from the critical temperature of the liquid−liquid equilibrium, i.e., $B = (\chi_c - A)T_c$. Although the choice of the *A* value may be empirical in determining the liquid−liquid coexistence region, the effect of χ is less significant for the nematic−nematic coexistence region. It should be pointed out that the *c* parameter

predominates in the phase diagram calculation of the nematic mixtures as compared to χ or molecular weight effects; these latter effects may become important in the liquid−liquid coexistence regions. The calculated phase diagram reveals the existence of two pure nematic regions (Figure 3), one being at the high E7 content (N_1) and the other being at the high concentration of EGDE-C6 (N_2). The two dotted lines are the peritectic lines which represent coexistence of three different phases consisting of two liquids plus one nematic or one liquid plus two nematics. There are two narrow nematic−liquid coexistence regions labeled $N_1 + L_2$ and $L_1 + N_2$. When the temperature reaches below the second peritectic line, a two-phase nematic region ($N_1 + N_2$) appears.

Figure 3b exhibits the cloud point temperature versus composition phase diagram of the EGDE-C7/E7 mixture in which the solid curves represent the calculated phase diagram using $c = 0.97$ and $r_2/r_1 = 5.44/1$. The theoretical phase diagram appears straightforward relative to that of the EGDE-C6/E6 system. At elevated temperatures, the system is isotropic and homogeneous. In the descending order of temperature, the system passes through an isotropic liquid−nematic coexistence region ($I + N$) into a single-phase nematic region (N). Upon further lowering of the temperature, two separated nematic phases ($N_1 + N_2$) are evident. The conventional critical point of the liquid−liquid equilibrium appears to be masked by the strong cross-nematic interaction.[11] A similar phase diagram had been observed by Finkelmann and co-workers[16] for a mixture of a low molar mass liquid crystal (4-(propyloxy)phenyl 4′-(hexyloxy)-benzoate) with a SCLCP (poly(dimethylsiloxane) grafted with a methoxyphenyl benzoate side group connected by a flexible spacer (four methylene units) to the backbone).

Figure 3c depicts the phase diagram of the EGDE-C8/E7 blend along with the theoretical curves (solid lines), calculated using $c = 0.94$ and $r_2/r_1 = 9/1$ (analogous to their molecular weight ratio). The phase diagram shown here is similar to that of the EGDE-C6/E7 system except that the two-phase nematic region ($N_1 + N_2$) moves to a higher temperature while the liquid−liquid ($L_1 + L_2$) region tends to diminish. The delicate competition between the Flory−Huggins χ and the Maier−Saupe ν_{jj} parameters probably decides the diminishing liquid−liquid region.[11] When the strength of cross-nematic interaction gets stronger, the liquid−liquid coexistence region gradually becomes smaller and finally is masked underneath the nematic region. Figure 3d shows the phase diagram of the EGDE-C9/E7 system. The solid lines were computed with $c = 0.96$ and $r_2/r_1 = 5.44/1$. It is striking to notice that this calculated phase diagram of the EGDE-C9/E7 closely resembles that of the EGDE-C7/E7 mixture.

To identify some of the coexistence regions, optical microscopic investigations were undertaken at the 30/70 and 40/60 EGDE-C6/C7 compositions. In Figure 4 are shown the microscopic pictures of the 30/70 EGDE-C6/E7 mixture at a slow cooling and heating rate of 0.5 °C/min. At 52 °C, both heating and cooling runs show a coexistence liquid−liquid phase since there is no identifiable anisotropic region under the polarized microscopic investigation. At 40 °C, the microscopic pictures exhibit a strong birefringent structure dispersed in a nonbirefringent matrix, indicating the existence of a nematic−liquid region. When temperature reaches 34 °C for the cooling (or 35 °C for the heating run), the strong birefringent patterns disappear; leaving only a few bright lines. The extinction of the

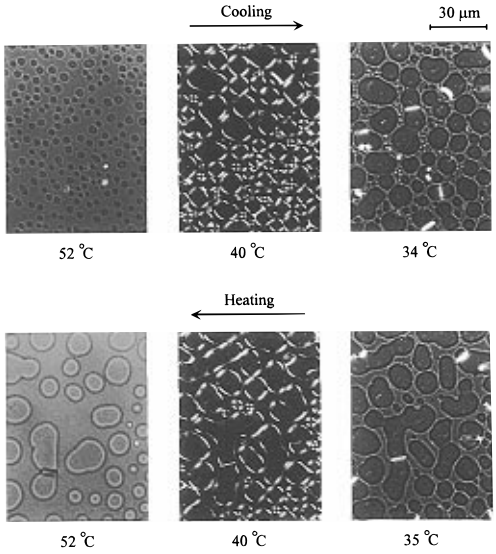

Figure 4. Structure evolution of the 30/70 EGDE-C6/E7 mixture during slow cooling and heating. The ramp rate was 0.5 °C/min.

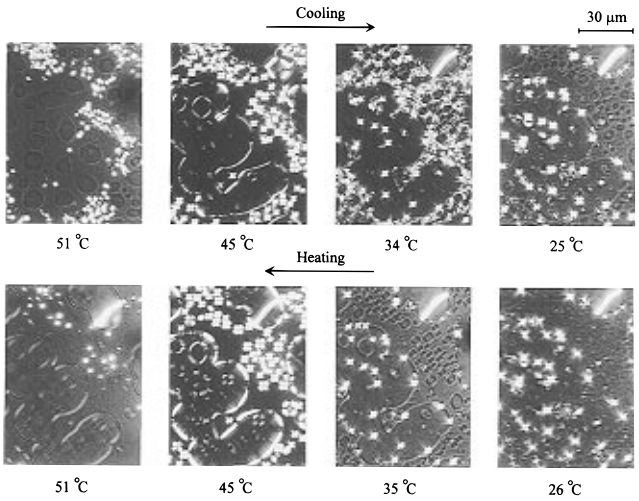

Figure 5. Structure evolution of the 40/60 EGDE-C6/E7 mixture during slow cooling and heating. The ramp rate was 0.5 °C/min.

birefringence may be attributed primarily to the homeotropic alignment of the dispersing liquid crystal molecules between two glass plates.[7] The residual bright lines are associated probably with the nematic defects. These structures are thermally reversible.

When the 40/60 EGDE-C6/E7 composition is cooled from an isotropic phase (70 °C), phase separation starts at 51 °C without encountering the liquid−liquid region (Figure 5). As can be expected, liquid−nematic phase separation occurs by showing strongly birefringent entities. The population of the birefringent entities reduces with continued cooling which may be driven by the homeotropic alignment of the LC molecules. The temperature is not low enough to reach the nematic−nematic coexistence region. To follow the nematic−nematic phase separation, a temperature quench experiment was conducted at the 40/60 composition from a single phase (70 °C) to about 18 °C close to the peritectic line. As can be seen in Figure 6, liquid−nematic phase separation first occurs for some initial period. Subsequently, the dark region gets brighter due to the nematic formation of the second component (presumably EGDE-C6), suggestive of the coexistence of two nematic phases. It seems that the peritectic line dividing the liquid−nematic and nematic−nematic re-

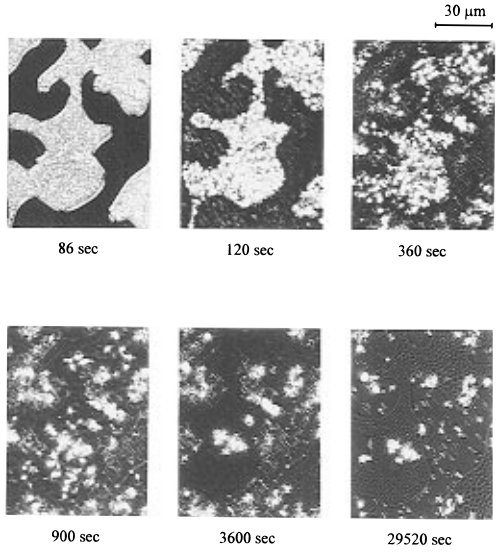

Figure 6. Time evolution of the structure in the 40/60 EGDE-C6/E7 mixture quenched from 70 to 18 °C.

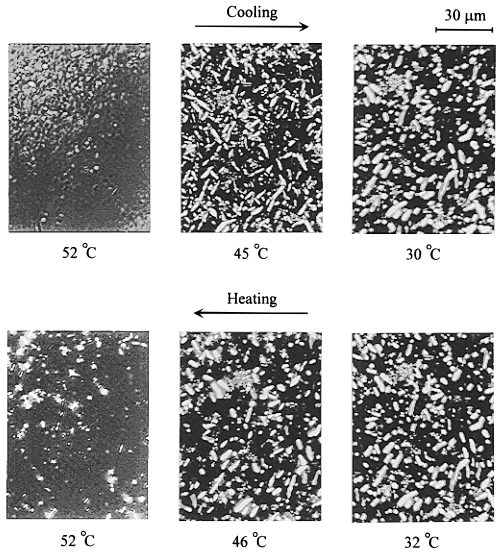

Figure 7. Structure evolution of the 50/50 EGDE-C7/E7 mixture during slow cooling and heating. The ramp rate was 0.5 °C/min.

gions may be underestimated for a few degrees. We believe that the same structure representing the coexistence of two nematics can be observed if the *T* quench was performed to a lower temperature (e.g. 15 °C or lower). Unfortunately, the present instrument was not designed for low-temperature experiments.

The identification of the coexistence regions of the EGDE-C7/E7 is by no means straightforward since the NI transition temperatures of the E7 and EGDE-C7 are very close. However, we are able to verify, if not all, some regions predicted by the combined FH/MS theory by carefully examining the microscopic pictures (taken during slow cooling) of the 50/50 EGDE-C7/E7 blend shown in Figure 7. At 52 °C, small nematic droplets emerge in the polymer matrix corresponding to an isotropic−nematic region. With a further decrease of temperature to 45 °C, the nematic textures display strong birefringence resembling schlieren textures. The birefringence tends to disappear at lower temperatures (e.g. 30 °C) which may be a consequence of the homeotropic alignment of the liquid crystalline molecules between two glass plates. Unfortunately, we cannot identify whether this nematic texture is representative of a single phase (N) or of a two-phase nematic (N_1 + N_2) region due to the proximity of the NI transition temperatures of the constituents. It seems reasonable to conclude that the two nematic coexistence region can be identified only if the NI transition temperatures of the constituent mesogens are sufficiently far apart (e.g., the EGDE-C6/E7 system in Figure 3a).

One striking feature of the nematic phase diagrams is the great similarity between the EGDE-C7/E7 and EGDE-C9/E7 and also the resemblance between the EGDE-C6/E7 and EGDE-C8/E7. It should be borne in mind that E7 is largely comprised of odd-numbered spacers (about 84%) mesogens. Hence, the mixtures such as EGDE-C7/E7 and EGDE-C9/E7 may be regarded as the odd−odd numbered spacer mixtures, showing a tendency of forming a single nematic in the phase diagram. By analogy, EGDE-C6/E7 and EGDE-C8/E7 may be considered as the even−odd-numbered spacer system that favors phase separation between two nematics. It is generally well accepted that the nematics of the odd-numbered spacers are less stable within their own phases relative to that of the even-numbered spacers. It is plausible that the nematics in the even-numbered spacer systems tend to be stabilized within their own species; therefore the even−even- or even−odd-numbered spacer mixtures may favor formation of separate nematic phases provided that there are no additional effects such as strong dipolar interaction, smectic ordering, or crystallization. On the other hand, the nematics in the odd−odd spacer systems could form either a single-phase nematic and/or two-phase nematics; the revelation of a narrow single-phase nematic gap in their phase diagrams points to this fact, although it is difficult to confirm experimentally.

The odd−even effect of the methylene spacers on the phase diagrams of the SCLCP/LC mixtures could be one of the major contributors, since other factors such as polarizability of mesogenic dipoles, spacer length, and chain rigidity, among others can influence the phase diagrams of their nematic mixtures. It is extremely difficult, if not impossible, to resolve the above individual contribution to the phase diagrams. At the present time, we felt that the phase diagrams of nematic mixtures may be best characterized by the "*c*" parameter, which is a measure of the strength of the cross-nematic interaction relative to that in their pure nematic phases, introduced by us.[11]

Dynamics of Phase Separation. Several temperature quenches were carried out at the 30/70 EGDE-C6/E7 mixture from a single temperature of 70 °C to a two-phase liquid−nematic region (25, 30, and 35 °C). The time evolution of scattering patterns associated with the domain within the liquid−nematic coexistence region (25 °C) is shown in Figure 8a,b. The scattering halo (Figure 8a) as evident under V_v (vertical polarizer with vertical analyzer) polarization may be attributed to the combined contributions of concentration fluctuations (liquid−liquid phase separation of the 30/70 EGDE-C6/E7 mixture) and orientation fluctuations (nematic ordering of the mesogens). The collapse of scattering halo to a smaller diameter is due to an increase of the length scale of concentration fluctuations during coarsening. The corresponding time evolution of H_v (horizontal polarizer with vertical analyzer) scattering is shown in Figure 8b. The H_v scattering arises exclusively from the orientation fluctuations. The initial cross-pattern appears to arise from rodlike entities such as liquid crystal aggregates. The center part of the H_v patterns is relatively strong, which may be contributed by the long range orientation fluctuations. With elapsed time, the rodlike scattering pattern gradually trans-

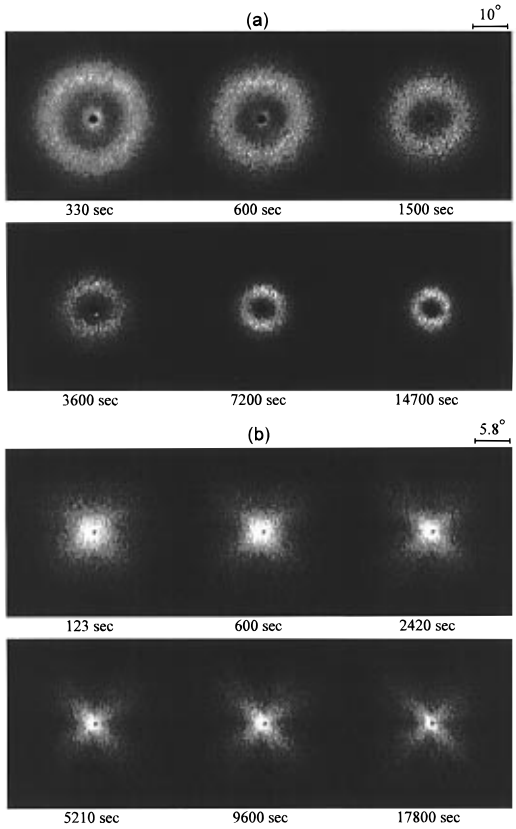

Figure 8. Time evolution of (a) V_v light scattering patterns and (b) H_v light scattering patterns of the 30/70 EGDE-C6/E7 mixture quenched from 70 to 25 °C.

forms to a shaper cross-pattern, although the scattering maximum appears to locate at the center. The H_v scattered intensity at later times decreases appreciably, which may be a consequence of the homeotropic alignment of LC molecules perpendicular to the two glass substrates. Visually, the overall size of the scattering patterns shows little or no change, except that the intensity increases. The monotonic decay of the H_v scattered intensity from the zero scattering angle has been observed in the 40/60 EGDE-C6/E7 and the 50/50 EGDE-C7/E7 systems when *T* quenches were performed directly into the nematic−nematic coexistence regions. It is extremely difficult, if not impossible, to estimate the size of orientation fluctuations without detecting a scattering maximum (rodlike scattering) under the H_v configuration. We, therefore, focus on the analysis of the V_v scattering contributed by the concentration fluctuations and by the orientation fluctuations.

Figure 9 shows the time evolution of scattering profiles (scattered intensity versus wavenumber maxima, q_m) of the 30/70 EGDE-C6/E7 mixture after quenching from 70 to 25 °C. The scattering wavenumber maximum shifts to a lower scattering angle with elapsed time while the intensity increases, suggestive of domain growth (dominated by the concentration fluctuation). A crossover of scattering curves can be discerned at larger wavenumbers, which implies that the smaller domains decay while the larger domains continue to grow. There is no indication of the early stage of spinodal decomposition where the scattering maxima ought to be stationary for some initial stages of phase decomposition.

The growth of the spinodal process has been customarily analyzed in the context of a power law[16−24] by examining the change of wavenumber maximum (q_m) and the corresponding peak intensity (I_m)

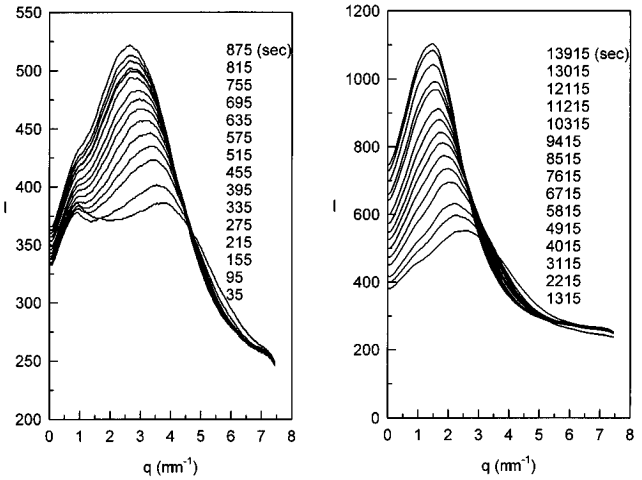

Figure 9. Time evolution of scattered intensity (*I*) versus wavenumber (*q*) of the 30/70 EGDE-C6/E7 mixture quenched from 70 to 25 °C.

$$q_m(t) \sim t^{-\alpha} \tag{20}$$

and

$$I_m(t) \sim t^{\beta} \tag{21}$$

where α and β are the growth exponents which have been predicted to be $^1/_3$ and 1 for late stages of spinodal decomposition in binary systems.[16−18]

Parts a and b of Figure 10 depict the log−log plots of $q_m(t) \sim t^{-\alpha}$ and $I_m(t) \sim t^{\beta}$, respectively, for three *T* quenches at the 30/70 EGDE-C6/E7 composition into the liquid−nematic region (25, 30, and 35 °C). At the *T* quench to 25 °C, the exponent value of α is approximately $^1/_8$ for some initial period, but it crosses over to $^1/_3$ at later times. The *T* quenches to 30 and 35 °C show an initial slope of $-^1/_8$, but the slope gets steeper with increasing elapsed time; i.e., the α value approaches approximately $^1/_2$. This growth behavior in the liquid−nematic coexistence is not appreciably different from the conventional liquid−liquid phase separation. It appears that orientation fluctuations associated with annihilation of nematic disclinations exert little or no effect on the coarsening dynamics, despite the fact that the wall effect and/or the nematic character of one component could alter the growth exponent. A similar exponent ($\alpha = ^1/_3$) was reported for a liquid crystalline polymer/polyester mixture.[20] The present observation is not surprising in view of the fact that the dynamics of annihilation of nematic disclinations in the pure small liquid crystals as well as in their mixtures have been shown to have comparable growth exponents ($\alpha = ^1/_3$[21] to 1[22]) relative to that of liquid−liquid phase separation.[18]

In the corresponding plots, the exponent β values at 25 °C are appreciably smaller than the relation of $\beta = 3\alpha$ predicted for flexible binary mixtures in the bulk. A similar trend is observed for the other two *T* quenches. The small exponent β values may be attributed to the reduced intensity caused by the homeotropic alignment of the LC molecules between the two glass substrates, as demonstrated earlier in Figures 4 and 5. This problem can be eliminated when the cover glass is not in use; e.g., the dynamics of phase separation in the liquid−nematic region of the mixtures of polystyrene/E7 as well as poly(methyl methacrylate)/E7 behaves the same way that is normally observed in the liquid−liquid phase separation, i.e., $\beta = 3\alpha$.[23−25]

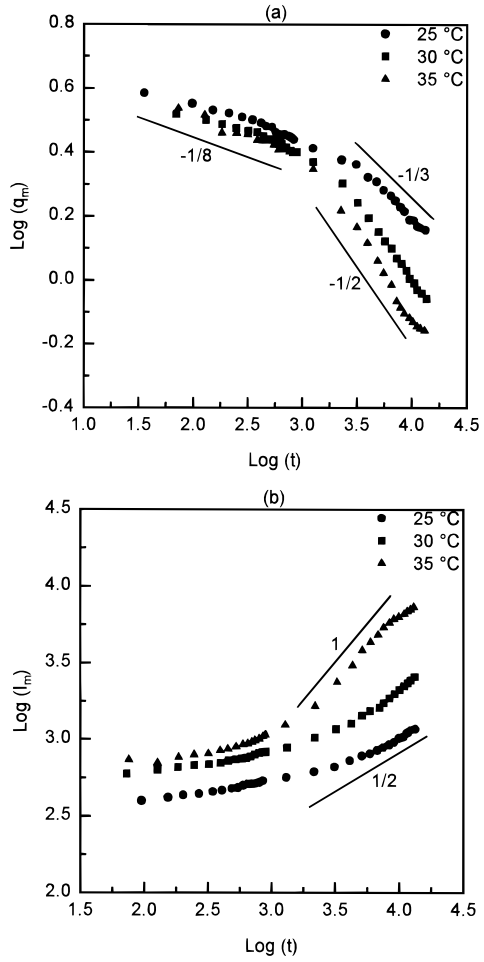

Figure 10. Double logarithmic plot of (a) scattered wavenumber maxima (q_m) versus elapsed time and (b) scattered intensity maxima (I_m) versus elapsed time for the 30/70 EGDE-C6/E7 mixture quenched from 70 °C to various temperatures.

In polymer blends, the surface wetting has been shown to exert a profound effect on the coarsening dynamics.[26] On the same token, the homeotropic alignment associated with surface anchoring and confinement effects of LC are expected to influence the dynamics of phase separation in the liquid−nematic region. However, the growth exponent (α) values turn out to be rather similar to those observed commonly in the liquid−liquid phase separation of binary mixtures[17,18] with exception that the β values are significantly smaller. The primary reason for this small β value may be due to the reduced scattered intensity caused by the homeotropic alignment of LC molecules between two glass substrates.

Conclusions

We have demonstrated that the combined FH/MS theory having two orientational order parameters and two clearing transition temperatures is capable of predicting various phase diagrams for nematic mixtures containing a side-chain liquid crystalline polymer as one component. The experimental phase diagrams were established for nematic mixtures of the eutectic small molecule liquid crystal (E7) and EGDE polymer backbone with an alkoxycyanobiphenyl group connected by various methylene linkages (C = 6−9). The FH/MS theory can fit the experimental phase diagram remarkably well. It is striking to observe a remarkable resemblance of the phase diagrams between the even−odd-numbered systems (EGDE-C6/E7 and EGDE-C8/E7) and also between the odd−odd-numbered systems (EGDE-C7/E7 and EGDE-C9/E7). This observation cannot be attributed exclusively to the odd−even effect of methylene spacers on the nematic−nematic phase diagrams because of other posible contributions arising from dipolar interaction of the mesogenic groups, the spacer length, and the rigidity of SCLCP. The dynamics of late stages of SD in the 30/70 EGDE-C6/E7 mixture show a crossover behavior of the scaling exponent α from $^1/_8$ to $^1/_3 \sim ^1/_2$ depending on the quench depth. We believe that the reduced scattered intensity caused by the homeotropic surface alignment of the LC molecules is one of the important contributors to the failure of the $\beta = 3\alpha$ relationship.

Acknowledgment. Support of this work by the NSF Science and Technology Center-ALCOM, Grant No. DMR 89-20147, is gratefully acknowledged.

References and Notes

(1) West, J. In *Liquid-Crystalline Polymers*; Weiss, R. A., Ober, C. K., Eds.; ACS Symp. Series No. 435; American Chemical Society: Washington, DC, 1990; Chapter 32, p 475.
(2) Doane, J. W. In *Liquid Crystals: Their Applications and Uses*; Bahadur, B., Ed.; World Scientific: New Jersey, 1990; p 361.
(3) Chien, L.-C.; Cada, L. G.; Xie, L. *Liq. Cryst.* **1992**, *12*, 853.
(4) Flory, P. J. *Principles of Polymer Chemistry*; Cornell University Press: Ithaca, NY, 1953.
(5) Olabisi, O.; Robeson, L. M.; Shaw, M. T. *Polymer-Polymer Miscibility*; Academic Press: New York, 1979.
(6) Maier, W.; Saupe, A. *Z. Naturforsch.* **1959**, *A14*, 882; **1960**, *A15*, 287.
(7) Chandrasekhar, S. *Liquid Crystals*, 2nd ed.; Cambridge University Press: Cambridge, U.K., 1992.
(8) de Gennes, P. G.; Prost, J. *The Physics of Liquid Crystals*, 2nd ed.; Oxford Science Publishers: London, 1993.
(9) Brochard, F.; Jouffroy, J.; Levinson, P. *J. Phys.* **1984**, *45*, 1125.
(10) Shen, C.; Kyu, T. *J. Chem. Phys.* **1995**, *102*, 556.
(11) Chiu, H.-W.; Kyu, T. *J. Chem. Phys.* **1995**, *103*, 7471.
(12) Smith, G. W. *Int. J. Mod. Phys.* **1993**, *B7*, 4187.
(13) Kyu, T.; Saldanha, J. M. *J. Polym. Sci., Polym. Lett. Ed.*, **1988**, *26*, 33.
(14) Gray, G. W. In *Molecular Structure and the Properties of Liquid Crystals*; Academic Press: New York, 1962; Chapter 9.
(15) Gray, G. W. In *Polymer Liquid Crystals*; Ciferri, A., Krigbaum, W. R., Theyer, R. B., Eds.; Academic Press: New York 1982; Chapter 1.
(16) Finkelmann, H.; Kock, H.-J.; Rehage, G. *Mol. Cryst. Liq. Cryst.* **1982**, *89*, 23.
(17) Gunton, J. D.; San Miguel, M.; Sahni, P. S. In *Phase Transitions and Critical Phenomena*; Domb, C., Lebowitz, J. L., Eds.; Academic Press: New York, 1983; Chapter 8, p 267.
(18) Binder, K.; Stauffer, D. *Phys. Rev. Lett.* **1973**, *33*, 1006.
(19) Siggia, E. *Phys. Rev. A* **1979**, *20*, 595.
(20) Shiwaku, T.; Nakai, A.; Hasegawa, H.; Hashimoto, T. *Polym. Commun.* **1987**, *28*, 174.
(21) Casagrande, C.; Veyssie, M.; Knobler, C. M. *Phys. Rev. Lett.* **1987**, *58*, 2079.
(22) Yurke, B.; Pargellis, A. N.; Turok, N. *Mol. Cryst. Liq. Cryst.* **1992**, *222*, 195.
(23) Kim, W.-K.; Kyu, T. *Mol. Cryst. Liq. Cryst.* **1994**, *250*, 131.
(24) Kyu, T.; Ilies, I.; Shen, C.; Zhou, Z. L. In *Recent Advances in Liquid Crystalline Polymers*; Isayev, A. I., Kyu, T.; Cheng, S. Z. D., Eds.; ACS Symposium Series; American Chemical Society: Washington, DC, in press.
(25) Kyu, T.; Ilies, I.; Mustafa, M. *J. Phys. IV* **1993**, *3*, 37.
(26) Cumming, A.; Wiltzius, P.; Bates, F. S. *Phys. Rev. Lett.* **1990**, *65*, 863.

MA951190E